[CANCER RESEARCH 64, 622–630, January 15, 2004]

Inhibition of *MUC4* Expression Suppresses Pancreatic Tumor Cell Growth and Metastasis

Ajay P. Singh,[1] Nicolas Moniaux,[1] Subhash C. Chauhan,[1] Jane L. Meza,[3] and Surinder K. Batra[1,2]

[1]Department of Biochemistry and Molecular Biology, [2]Eppley Institute for Research in Cancer and Allied Diseases, and [3]Department of Preventive and Societal Medicine, Biostatistics Section, University of Nebraska Medical Center, Omaha, Nebraska

ABSTRACT

The MUC4 mucin is a high molecular weight membrane-bound glycoprotein. It is aberrantly expressed in pancreatic tumors and tumor cell lines with no detectable expression in the normal pancreas. A progressive increase of *MUC4* expression has also been observed in pancreatic intraepithelial neoplasia, suggesting its association with disease development. Here, we investigated the consequences of silencing *MUC4* expression in an aggressive and highly metastatic pancreatic tumor cell line CD18/HPAF that expresses high levels of MUC4. The expression of *MUC4* was down-regulated by the stable integration of a plasmid-construct expressing antisense-MUC4 RNA. A decrease in MUC4 expression, confirmed by Western blot and immunofluorescence analyses, resulted in diminished growth and clonogenic ability of antisense-MUC4-transfected (EIAS19) cells compared with parental, empty vector (ZEO) and sense transfected (ES6) control cells. In addition, EIAS19 cells displayed a significant decrease in tumor growth and metastatic properties when transplanted orthotopically into the immunodeficient mice. *In vitro* biological assays for motility, adhesion, and aggregation demonstrated a 3-fold decrease in motility of EIAS19 cells compared with control cells, whereas these cells adhered more and showed an increase in cellular aggregation. Interestingly, *MUC4* down-regulation also correlated with the reduced expression of its putative interacting partner, HER2/neu, in antisense-MUC4-transfected cells. In conclusion, the present work demonstrates, for the first time, a direct association of the MUC4 mucin with the metastatic pancreatic cancer phenotype and provides experimental evidence for a functional role of MUC4 in altered growth and behavioral properties of the tumor cell.

INTRODUCTION

Pancreatic cancer is the fourth leading cause of cancer-related deaths in the United States (1). It is characterized by extensive local invasion into surrounding tissues and early hematogeneous and lymphatic metastasis to distant organs, resulting in a poor prognosis for the patients (2). At the time of diagnosis, >80% of patients have locally advanced or metastatic disease. The overall median survival time after diagnosis is 2–8 months, and only 1–4% of all patients with adenocarcinoma of the pancreas survive 5 years after diagnosis (2, 3). The inability to detect cancer at an early stage, aggressiveness of the disease, and the lack of effective systemic therapies for the treatment are largely responsible for the rapid death and low survival of the patients. Hence, the efforts to gain information on the pathobiology of pancreatic cancer and to elucidate the molecular mechanisms related to the invasion/metastasis of the tumor cells are urgently needed for developing novel and effective therapeutic approaches for treatment.

Mucins, in general, play a protective role for the adjoining epithelial tissues under normal physiological conditions (4, 5), whereas an altered expression of mucins is often associated with carcinomas and neoplastic lesions (6). The involvement of mucins in the renewal and differentiation of the epithelium, as well as in the modulation of cell adhesion and in cell signaling, has also been proposed (7–9). In an extensive study on mucin gene expression, we have demonstrated a specific and differential expression pattern of *MUC4* in pancreatic adenocarcinoma and tumor cell lines compared with the normal pancreas and pancreatitis (10). Furthermore, in recent studies, a progressive increase in *MUC4* expression has been observed in pancreatic intraepithelial neoplastic lesions (11, 12), indicating its role in disease development. The up-regulation of *MUC4* in several other human adenocarcinomas (13–16) also indicates the potential importance of this mucin in tumor biology.

MUC4 mucin is a high molecular weight glycoprotein that belongs to the family of membrane-bound mucins. The *MUC4* gene has been cloned from a human tracheobronchial cDNA library (17, 18) and from the human pancreatic tumor cell line (19). The NH_2 terminus of the MUC4 protein is composed of a 27 amino acid signal peptide, followed by a unique sequence of 951 residues and a large tandem repeat domain varying in length from 3285 to 7285 amino acid residues because of a variable number of tandem repeats. The COOH terminus of MUC4 consists of a 1156-residue peptide and includes two cysteine-rich domains, three epidermal growth factor-like domains, a hydrophobic transmembrane region, and two regions rich in potential *N*-glycosylation sites (17). Depending on the size of the central tandem repeat domain, the molecular weight of the nascent protein may range from M_r 550,000 to M_r 930,000. MUC4 is considered to be a human homologue of rat sialo-mucin complex (SMC, rat Muc4) because of similarities in structural organization. SMC is a heterodimeric glycoprotein composed of an *O*-glycosylated mucin subunit, ascites sialoglycoprotein (ASGP-1), tightly bound to a *N*-glycosylated transmembrane subunit, ASGP-2, which contains two epidermal growth factor-like domains in its extracellular part. In a similar way, MUC4 may also be cleaved into two subunits: the mucin subunit MUC4α and a transmembrane subunit MUC4β with three epidermal growth factor-like domains (5, 17). SMC has previously been shown to facilitate tumor development/progression by multiple mechanisms (7, 20, 21). The mucin type ASGP-1 subunit of SMC confers antiadhesive and immunosuppressive properties to the tumor cell (20, 22), while the transmembrane ASGP-2 subunit has been shown to act as an intramembrane ligand for the receptor tyrosine kinase ErbB2 via one of its two epidermal growth factor-like domains, leading to its phosphorylation (23). The *ErbB2/HER2/neu* gene is a member of the ErbB-like oncogene family, and its overexpression has been associated with increased cell proliferation and the development of metastatic disease (24). Studies conducted in our laboratory have shown that MUC4 and HER2 interact with each other and colocalize at the cell surface and in cytoplasm (unpublished data). However, it is not yet well defined whether such interaction may also lead to HER2/neu phosphorylation and its downstream signaling.

In the present study, we elucidated the role of MUC4 in tumor cell growth, behavior, and metastasis in a human pancreatic adenocarcinoma cell line CD18/HPAF, using *in vitro* biological assays and *in vivo*, in an orthotopic mouse model of pancreatic cancer. *MUC4* expression was knocked down in CD18/HPAF cells by the stable

Received 8/22/03; revised 10/3/03; accepted 11/5/03.

Grant support: R01 Grant CA78590 from the NIH.

The costs of publication of this article were defrayed in part by the payment of page charges. This article must therefore be hereby marked *advertisement* in accordance with 18 U.S.C. Section 1734 solely to indicate this fact.

Requests for reprints: Surinder K. Batra, Department of Biochemistry and Molecular Biology and Eppley Institute, University of Nebraska Medical Center, 984525 Nebraska Medical Center, Omaha, Nebraska 68198-4525. Phone: (402) 559-5455; Fax: (402) 559-6650; E-mail: sbatra@unmc.edu.

transfection of an antisense RNA construct to *MUC4*. Our results demonstrate, for the first time, the direct association of the MUC4 mucin with pancreatic tumor cell growth and metastasis and suggest a novel feature of MUC4 in regulating HER2/neu expression.

MATERIALS AND METHODS

Construction of Plasmids Expressing MUC4 Antisense RNA. Two partial length MUC4 DNA fragments, *Eco*RI51688-*Bam*HI52286 (AC025282) and *Eco*RI390-*Bam*HI689 (AJ000281), were obtained through PCR amplification using a DNA template from the S1243 MUC4 clone (18). The fragment *Eco*RI51688-*Bam*HI52286 covered a 598-bp region from Exon1 and Intron1, whereas fragment *Eco*RI390-*Bam*HI689 contained a 300-bp stretch from exon1 only. The two fragments were cloned in antisense orientation behind the cytomegalovirus promoter of the pcDNA3.1/zeo$^+$ vector from Invitrogen (San Diego, CA), using standard recombination techniques. The fragment *Eco*RI390-*Bam*HI689 was also cloned in sense orientation to serve as a control. The resulting three constructs were designated pcDNA3.1-ES ($exon_1$ sense), pcDNA3.1-EAS ($exon_1$ antisense), and pcDNA3.1-EIAS ($exon_1$-$intron_1$ antisense). The insert sequence and orientation were confirmed by sequencing of the recombinants.

Cell Culture and Transfection. CD18/HPAF cells were cultured in DMEM:Ham's F12 (1:1) supplemented with 10% FCS and antibiotics (100 μg/ml penicillin and streptomycin). Cells were grown at 37°C with 5% CO_2 in a humidified atmosphere. CD18/HPAF cells were stably transfected with pcDNA3.1/zeo vector containing sense and antisense inserts or containing no insert using Lipofectamine (Invitrogen), following the manufacturer's protocol. The zeocin-resistant colonies were isolated by the ring cloning method and maintained in medium supplemented with 200 μg/ml zeocin (Invitrogen). Medium was replaced with complete medium without antibiotic supplement at least 5 days before any analysis.

Reverse Transcription-PCR. *MUC4* gene specific primers flanked with *Eco*RI and *Bam*HI restriction site sequences were synthesized at the Molecular Biology Core Facility at University of Nebraska Medical Center. The primer sequences were: forward-CGCGAATTCTCTGCTCCTCACACTGCA (*MUC4* $exon_1$ and $exon_1$-$intron_1$ segment), reverse-CGCGGATCCGGTTCTGAGATGAAGCTG (*MUC4* $exon_1$ segment), and reverse-CGCGGATCCCAGACTCCTGAGTAGCTGG (*MUC4* $exon_1$-$intron_1$ segment). To analyze the expression of inserts in the transfected cell lines, 2 μg of RNA were reverse transcribed and amplified using standard primers (T7, forward; BGH, reverse). Additionally, the orientation of the transcribed insert was verified using a combination of vector-specific (T7 or BGH rev) and insert-specific primers. Reverse transcription-PCR was performed as described previously (25).

Immunoblot Assay. The CD18/HPAF and derived cell lines were processed for protein extraction and Western blotting using standard procedures. Briefly, the cells were washed twice in PBS and scraped in radioimmunoprecipitation assay buffer [50 mM Tris, 5 mM EDTA, 150 mM NaCl, 0.25% sodium deoxycholate; 1% NP40 (pH 7.5)], supplemented with protease inhibitor mixture (Roche Diagnostics, Mannheim, Germany) and phosphatase inhibitors (5 mM NaF and 5 mM Na_3VO_4; Sigma Chemicals, St. Louis, MO), and kept at 4°C for at least 30 min. Cell lysates were passed through the needle syringe or alternatively subjected to one freeze thaw cycle to facilitate the disruption of the cell membranes. Cell lysates were centrifuged at 14,000 rpm for 20 min at 4°C, and supernatants were collected. Protein concentrations were determined using a BIO-$RAD_{D/C}$ protein estimation kit. Because of the large size of MUC4, the proteins (10 μg) were resolved by electrophoresis on a 2% SDS-agarose gel under reducing conditions. For phosphoglycerol kinase and HER2/neu expression analysis, SDS-PAGE (10%) was run under similar conditions. Resolved proteins were transferred onto the polyvinylidene difluoride membrane and subjected to the standard immunodetection procedure using specific antibodies: antihuman phospho-glycerol kinase (used as internal control); anti-HER2; and anti-phosphotyrosine^{1248}-HER2 (all rabbit polyclonal; Cell Signaling Technology, Beverly, MA). For MUC4 immunodetection, anti-MUC4 mouse monoclonal antibody (8G7) was used, which has been generated in our laboratory and has been used reliably in previous studies (11, 12). Secondary antibodies consisted of horseradish peroxidase-conjugated goat antimouse (for MUC4) and antirabbit (for phosphoglycerol kinase, HER2 and phosphotyrosine^{1248}-HER2; Amersham Biosciences, Buckinghamshire, United Kingdom). The blots were processed with ECL Chemiluminescence kit (Amersham Biosciences), and the signal was detected by exposing the processed blots to X-ray films (Biomax Films, Kodak, NY).

Confocal Immunofluorescence Microscopy. For immunofluorescence labeling, cells were grown at low density on sterilized coverslips for 20 h. After washing with 0.1 M HEPES containing Hanks buffer, the cells were fixed in ice-cold methanol at −20°C for 2 min. Nonspecific blocking was done in 10% goat serum containing 0.05% Tween 20 for at least 30 min, followed by incubation with the anti-MUC4 monoclonal antibody (8G7) in PBS for 90 min at room temperature. Cells were washed 4 × 5 min with PBS containing 0.05% Tween 20 (PBS-T) and then incubated with FITC-conjugated goat antimouse secondary antibodies for 60 min. Cells were washed twice with PBS-T and mounted on glass slides in antifade Vectashield mounting medium (Vector Laboratories, Burlingame, CA). Immunostaining was observed under a ZEISS confocal laser-scanning microscope, and representative photographs were captured digitally using 510 LSM software.

Growth Kinetics Assay. Cells (10^4 cells/3 ml medium) were seeded in 6-well plates and allowed to grow for different times. The growth rate was determined by counting the number of cells on a hemocytometer in triplicate on every day of culture up to the seventh day. Cell population doubling time (T_d) was calculated during exponential growth phase (96–144 h) using the following formula (26): $T_d = 0.693\ t/ln\ (N_t/N_0)$, where t is time (in h), N_t is the cell number at time t, and N_0 is the cell number at initial time.

Colony-Forming Assay. Cells were seeded in triplicate at 500 cells/10-cm dishes in complete medium. After 2 weeks of growth, the cells were fixed and stained with crystal violet stain (0.1%, w/v) in 20 nM 4-morpholinepropanesulfonic acid (Sigma Chemicals), and the grossly visible colonies were counted. All experiments were repeated at least three times. Plating efficiency was determined as the number of colonies formed, divided by the total number of cells plated.

Tumorigenicity Assay. To test the tumorigenic capacity, antisense-transfected CD18/HPAF cells along with the control cells were harvested from subconfluent cultures by a brief exposure to 0.25% trypsin and 0.02% EDTA. Trypsinization was stopped with medium containing 10% fetal bovine serum, and the cells were washed once in PBS. Cell viability and count were determined by trypan blue staining using hemocytometer. Cells were resuspended in a normal saline solution at a concentration of 5×10^6 cells/ml. Single-cell suspensions of >90% viability were used for the injections.

Immunodeficient mice were purchased from the Animal Production Area of the National Cancer Institute-Frederick Cancer Research and Development Center (Frederick, MD). The mice were housed in specific pathogen-free conditions and were fed sterile water and food *ad libitum*. The mice were treated in accordance with the Institutional Animal Care and Use Committee guidelines. The mice (8–12 weeks old) were anesthetized with 350 μl of i.p. injection of a mixture (4:1) of ketamine (100 mg/ml) and xylazine (20 mg/ml) diluted 10 times in sterile water. A small left abdominal flank incision was made, and the spleen was exteriorized. Tumor cells (5×10^5) were injected subcapsularly in a region of the pancreas just beneath the spleen using a 1-cc U-100 insulin disposable syringe (Becton Dickinson, Franklin Lakes, NJ). A successful subcapsular intrapancreatic injection of tumor cells was identified by the appearance of a fluid bleb without i.p. leakage. To prevent leakage, a cotton swab was held for 30–60 s over the site of injection. Wounds were closed by making a single suture on one layer and three to five independent sutures on the outermost skin. Tumor growth was assessed by the daily weighing and palpation of each animal. All mice were sacrificed on day 21 after implantation, and the presence of metastatic lesions in different organs was determined. Pancreatic tumors were excised, weighed, and measured for their dimensions.

Immunohistochemistry. Frozen pancreatic tumor tissues from the sacrificed mice were embedded in OCT compound (Sakura Fine Technical Co., Tokyo, Japan), and 5-μm thick cryosections were prepared on LEICA CM 1850 cryostat. Sections were mounted on Superfrost positively charged glass slides and processed for immunohistochemistry using an ABC kit (Vector Laboratories) according to the manufacturer's protocol with slight modifications. Briefly, frozen sections were kept at room temperature for 10 min followed by 10 min of incubation in PBS before methanol fixation. Nonspecific binding was blocked by incubating the sections with normal goat-serum for 30 min at room temperature. Endogenous peroxidase activity was quenched by incubating sections in 3% H_2O_2 in PBS for 20 min. Sections were then

incubated with anti-MUC4 monoclonal antibody for 30–60 min at room temperature and washed with PBS-T (3 × 5 min) before incubating with secondary antibody for 30 min. Slides were washed again (3 × 5 min) with PBS-T before incubating with the ABC solution. The reaction color was developed by incubating sections with 3,3′-diaminobenzidine reagent. The slides were washed with water and counterstained with hematoxylin. The sections were then dehydrated and mounted with Permount permanent mounting media (Fisher Scientific, Fair Lawn, NJ). All slides were observed under Nikon E400 Light Microscope and representative photographs were taken.

Adhesion Assay. Adhesion to an uncoated surface was performed using a 24-well plate. Cells were starved overnight, trypsinized, and resuspended in DMEM containing 10% FBS. Cells (2×10^5) were plated in each well and allowed to attach for 5 h at 37°C. Shorter incubation time (5 h) was chosen to avoid differences that may arise because of differential growth kinetics. Floating cells were carefully aspirated, transferred to tubes, and spun, and both plates and tubes were washed with PBS and fixed in 5% formaldehyde. The fixed cells were then washed and allowed to dry. Dried fixed cells were stained using crystal violet (0.1%, w/v) in 20 nM 4-morpholinepropanesulfonic acid (Sigma Chemicals) and then solubilized using 200 μl of 10% acetic acid. Absorbance (at 590 nm) was measured using an ELISA reader.

Aggregation Assay. Cells were tested for their ability to aggregate in hanging drop suspension cultures. Cells were trypsinized in the presence of EDTA, washed twice in PBS, and resuspended at 2.5×10^5 cells/ml in the appropriate medium containing 10% FBS. Drops (20 μl each) of medium, containing 5000 cells/drop, were pipetted onto the inner surface of the lid of a Petri dish. The lid was then placed on the Petri dish so that the drops were hanging from the lid with the cells suspended within them. To eliminate evaporation, 8 ml of serum-free culture medium were placed in the bottom of the Petri dish. After overnight incubation at 37°C, the lid of the Petri dish was inverted and photographed using a Nikon TS100 inverted tissue culture microscope at ×40 magnification.

Motility Assay. For motility assays, 1×10^6 cells were plated in the top chamber of noncoated polyethylene teraphthalate membranes (6-well insert, pore size 8 mm; Becton Dickinson). The cells were incubated for 24 h, and the cells that did not migrate through the pores in the membrane were removed by scraping the membrane with a cotton swab. Cells that transversed the membrane were stained with a Diff-Quick cell staining kit (Dade Behring, Inc., Newark, DE). Cells in 10 random fields of view at ×100 magnification were counted and expressed as the average number of cells/field of view. Three independent experiments were done in each case. The data were represented as the average of the three independent experiments with the SD of the average indicated.

Statistical Analyses. Statistical analyses were performed using SAS software (SAS Institute, Carey, NC). The Mann-Whitney *U* test was used to compare tumor weight and tumor volume between groups. Fisher's exact test was used to compare the frequency of metastasis between groups. $P < 0.05$ was considered to be statistically significant.

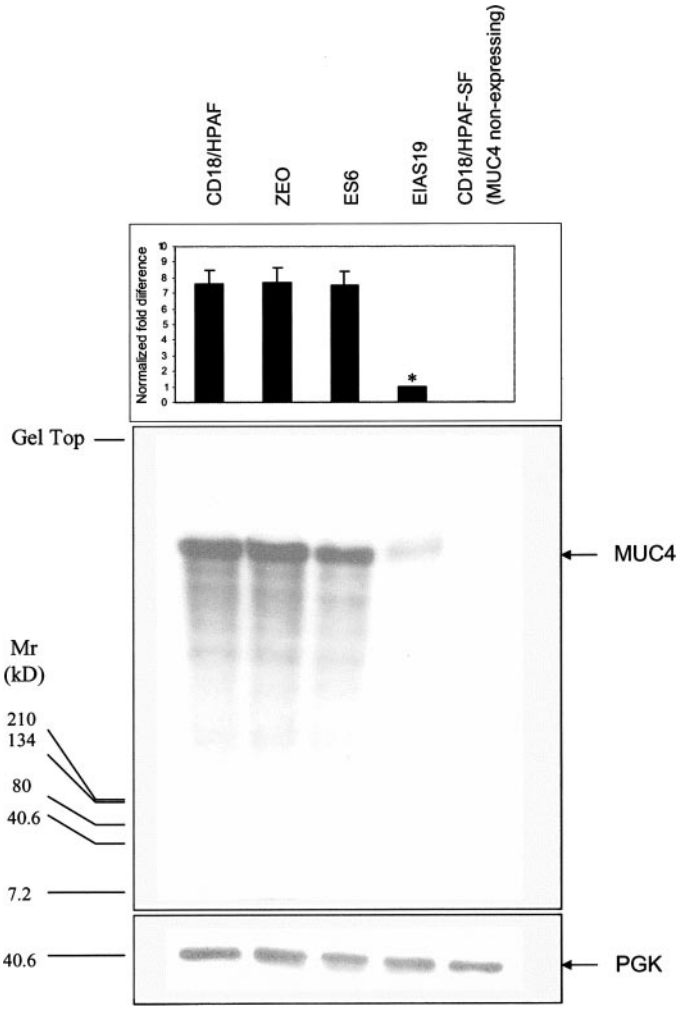

Fig. 1. Western blot analysis of MUC4 expression in CD18/HPAF and its derived sublines: ZEO (empty vector transfected), ES6 (MUC4-exon$_1$ sense transfected), and EIAS19 (MUC4-exon$_1$-intron$_1$ antisense transfected). A total of 10 μg protein from cell extracts was resolved by electrophoresis on a 2% SDS-agarose gel, transferred to polyvinylidene difluoride membrane, and incubated with anti-MUC4 monoclonal antibody. The membrane was then probed with horseradish peroxidase-labeled goat antimouse immunoglobulin. Immunoblot of phosphoglycerol kinase (*PGK*), obtained from 10% SDS-PAGE/Western, was used as an internal control to correct for the loading variation. The signal was detected using an electrochemiluminescence reagent kit. MUC4 mucin is a high molecular weight glycoprotein and the predicted size of the unglycosylated protein is M_r 930,000 [M_r 850,000 (MUC4α) and M_r 80,000 (MUC4β)]. Glycosylation can further add 3–5 folds to the mature protein molecular weight. *Bars* represent the normalized fold difference in MUC4 protein expression levels (mean ± SE; $n = 3$, *, $P < 0.05$).

RESULTS

Characterization of CD18/HPAF-Derived Transfected Sublines for *MUC4* Expression. A total of 23 single cell clones [3 empty vector (ZEO), 6 exon$_1$-sense construct (ES), 5 exon$_1$-antisense (EAS), and 9 exon$_1$-intron$_1$-antisense (EIAS) transfected] was selected upon growing the cells in zeocin containing media. The insertion, orientation, and expression of inserts were determined by reverse transcription-PCR using the vector and insert-specific PCR primers (data not shown). *MUC4* expression in the derived sublines was examined via Western blot analysis. All of the clones expressing antisense-MUC4 transcripts showed a 30–90% reduction in MUC4 protein. The selected antisense sublines were monitored over a period of 2–3 months for the stability and consistent diminished expression of *MUC4*. A clonal antisense subline, EIAS19, that showed approximately up to 80–90% reduction of MUC4 in repetitive experiments (Fig. 1) was selected for additional *in vitro* and *in vivo* studies, along with the randomly picked clones from empty vector-transfected (ZEO) and sense-transfected (ES6) CD18/HPAF cells, to determine the role of MUC4 in tumor development and progression. Results of the confocal immunofluorescent microscopy were also consistent with Western blot analysis, which confirmed the reduced cellular expression of MUC4 in EIAS19 cells compared with control cells (Fig. 2).

Reduced *MUC4* Expression Affects Growth Characteristics of CD18/HPAF Cells. To determine any changes occurring in the cell growth pattern and morphology due to reduced *MUC4* expression, cells were seeded at low density (5×10^6 cells/75-cm^2 flask) and observed under optical microscope every day until they reached confluency. Antisense-transfected EIAS19 cells grew slower and formed adherent clumps compared with the controls that displayed a more random and disperse growth pattern (Fig. 3). No changes, however, were observed in their morphology (at low confluence) compared with that of the control cell lines. We additionally examined whether the down-regulation of *MUC4* influenced the growth of CD18/HPAF cells. Growth rates were determined for parental CD18/HPAF and its derived cell lines by cell counting in a Coulter counter

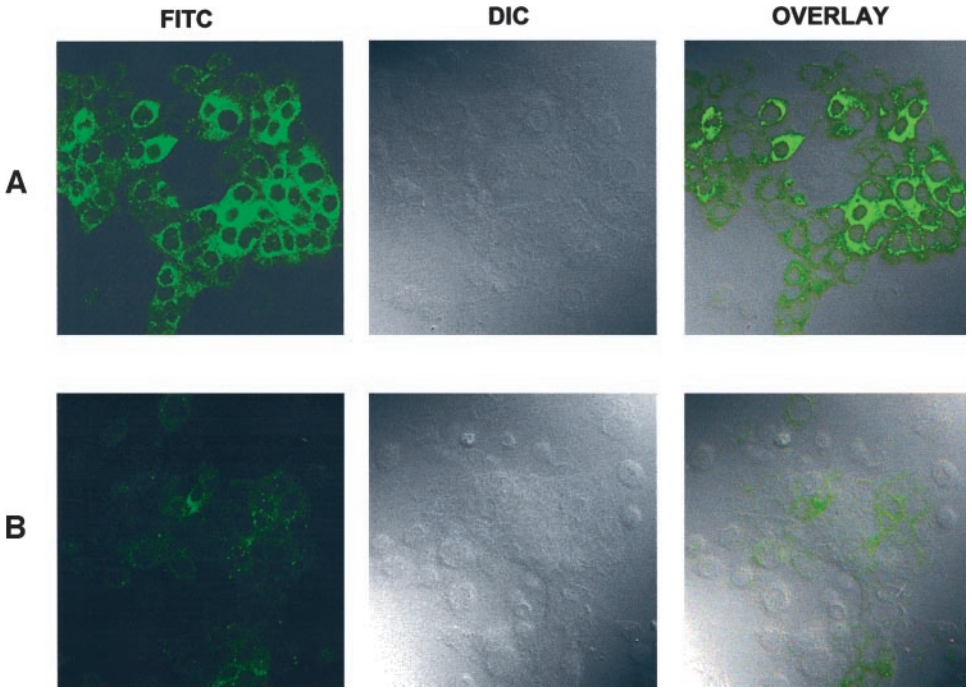

Fig. 2. Expression analysis of MUC4 using confocal microscopy. Empty vector-transfected CD18/HPAF (ZEO; *A*) and antisense MUC4-transfected (EIAS19; *B*) cells. Cells were grown at low density on sterilized coverslips, washed, and fixed in ice-cold methanol at −20°C. After blocking in 10% goat serum, cells were incubated with the anti-MUC4 mouse monoclonal antibody, washed, and followed by secondary incubation with FITC-conjugated goat antimouse IgG. Cells were mounted on glass slides in antifade Vectashield mounting medium before observation under a ZEISS confocal laser scanning microscope (magnification, ×630).

and/or by hemocytometer at different time intervals (Fig. 4*A*). When the cell numbers were compared on day 7, the antisense-transfected cells (EIAS19) showed 26–33% inhibition of growth compared with CD18/HPAF, empty vector (ZEO), and sense (ES6) controls. Population doubling times were calculated from cell growth during exponential phase (96–144 h). EIAS19 cells displayed a significant increase in doubling time ($P < 0.05$) of 24 h compared with the control cells, which had doubling times of ≈19 h (Fig. 4*B*).

Plating efficiency is a measure of the clonogenic ability of cells. Cancer cells, in general, have higher plating efficiencies than normal cells. Plating efficiencies of CD18/HPAF and derived sub-lines were assessed by seeding 500 cells in a 60-mm culture dish and counting the grossly visible colonies after two weeks. EIAS19 cells showed a significant decrease (22–29%) in plating efficiency compared with the controls (Fig. 5). Altogether, these observations suggest that dysregulated *MUC4* expression in pancreatic cancer may be implicated in tumor cell growth.

Down-Regulation of MUC4 Results in Reduced Tumorigenicity and Metastasis of the CD18/HPAF Cells. To test the hypothesis that MUC4 plays a role in tumor development and potentiation of tumor metastasis, we examined the changes in the tumorigenicity and metastatic potential of antisense MUC4-transfected CD18/HPAF cells *in vivo*. A total of 4–6 immunodeficient mice was orthotopically injected with antisense-transfected (EIAS19), vector-transfected (ZEO), sense-transfected (ES6) and parental CD18/HPAF cells in three different sets of experiments and sacrificed on day 21 after injection. Primary tumors were resected, and data were recorded for tumor weight and volume (Table 1). The incidence of metastases present on the distant organs, including the liver, lung, diaphragm, intestine, kidneys, lymph nodes, and heart were also documented (Table 2). All of the mice injected with the CD18/HPAF controls or antisense construct-transfected (EIAS19) cells developed primary tumors. Tumors developed from the EIAS19 cells were significantly smaller ($P = 0.01$) measuring a median weight of ~50–58% to that of the control tumors (Table 1). Also, a 35–43% reduction in median tumor volume was observed (Table 1). Most (94%) of the 36 control mice developed metastases at one to multiple sites, whereas only 31% (4 of 13) of the low MUC4 expressing primary tumors had detectable metastases (Table 2). Specifically, the incidence of lymph node metastasis was lower in the EIAS19 cells compared with CD18/HPAF ($P = 0.02$), ZEO ($P < 0.001$), and ES6 ($P < 0.001$). The incidence of diaphragm metastases was also lower in the EIAS19 cells compared with CD18/HPAF ($P < 0.001$) and ZEO ($P = 0.04$). Immunohistochemical analysis of the primary tumor tissue sections was performed with the anti-MUC4 antibody. Staining confirmed the presence of metastatic cells and relatively low MUC4 expression in antisense-construct-transfected cells (Fig. 6).

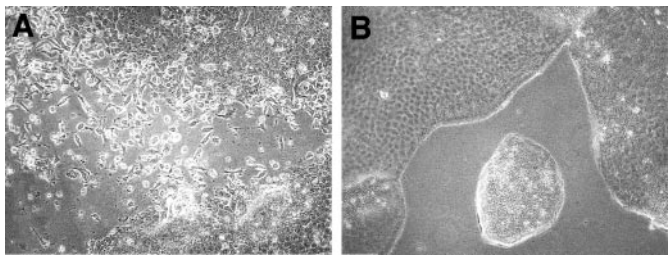

Fig. 3. Phase contrast micrograph of empty vector-transfected CD18/HPAF (ZEO; *A*) and antisense MUC4-transfected (EIAS19; *B*) cells to analyze cell's growth pattern *in vitro*. Cells were seeded at low density (1×10^6 cells in 75-cm^2 flasks) and grown in culture media [DMEM:Ham's F12 (1:1) + 10% FBS]. The present phase contrast picture was taken at ~80% confluence with respect to control (ZEO) cells. Antisense-MUC4 transfected (EIAS19) cells grew slower and in adherent clumps compared with a fast and random growth pattern of other control cells.

Aggregation and Adhesion Are Enhanced, and Motility Is Decreased in CD18/HPAF Cells Stably Transfected with Antisense-MUC4 Construct. A variety of phenotypic characteristics are required for a cancer cell to successfully complete the metastatic cascade. Among these, acquisition of a motile phenotype is one requirement for a cell to become metastatically competent. The other factors that may critically affect tumor cell metastasis are aggregation and adhesive properties of the cells. These properties are usually altered in the tumor cells either because of direct changes in the expression of cell surface adhesion molecules or because of changes in the other membrane proteins that can potentially disrupt the interaction between these adhesion molecules (22, 27, 28). Therefore, we

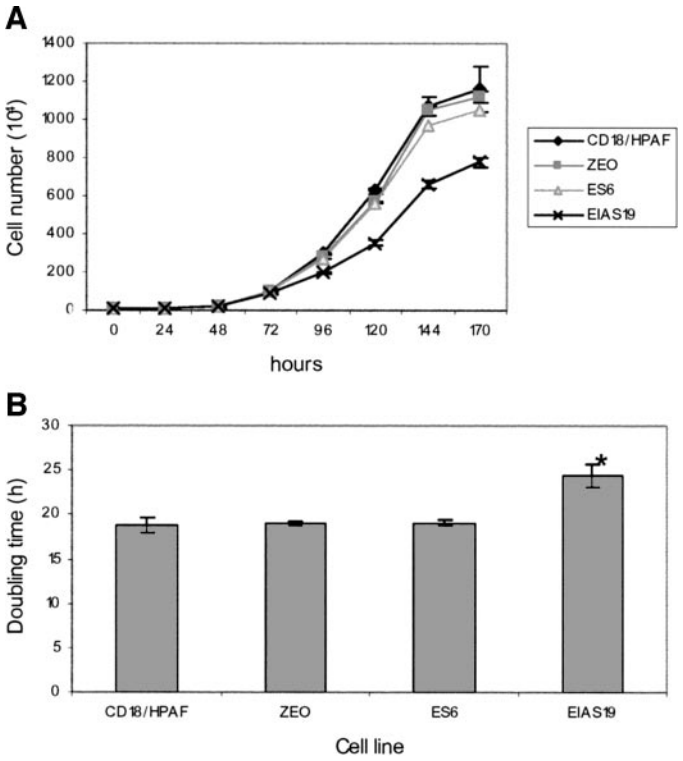

Fig. 4. Growth kinetics of EIAS19 (antisense-MUC4 transfected) cells compared with CD18/HPAF and derived control cell lines. *A*, growth curve plotted for cell number *versus* time of incubation of tumor cells *in vitro*. A total of 10×10^4 cells was seeded at 0 h, and increases in cell number in different cell lines were determined at an interval of 24 h up to 7 days. Mean ± SE; $n = 3$. *B*, cell population doubling time. Doubling time was calculated from the cell growth curve during the exponential growth phase (96–144 h) according to the equation $T_d = 0.693t/\ln(N_t/N_0)$, where t is time (in h), N_t is the cell number at time t, and N_0 is the cell number at initial time. Mean ± SE; $n = 3$; *, $P < 0.05$.

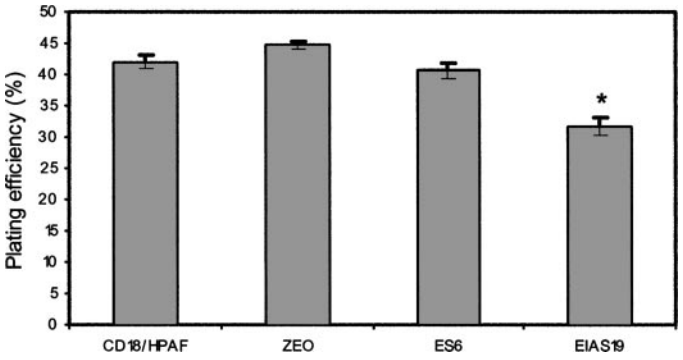

Fig. 5. Cell-plating efficiency of the MUC4-expressing and the MUC4-knockdown CD18/HPAF tumor cells. Five hundred cells were seeded in 10-cm dishes and grown for 2 weeks. Cells were fixed and stained with 0.1% crystal violet and the grossly visible colonies were counted. Mean ± SE; $n = 3$; *, $P < 0.05$. MUC4 knockdown cells (EIAS19) displayed a lower plating efficiency compared with control cells.

sought to determine whether reduced expression of MUC4 would influence the adhesion, aggregation, and motility of the CD18/HPAF cells. Cell motility was determined onto the uncoated porous membrane. The number of cells migrated to the lower surface of the porous membrane was ~3-fold greater in MUC4-expressing control cells (ZEO) than that of *MUC4*-silenced EIAS19 cells (Fig. 7*A*). This difference persisted and increased additionally over a period of 48 h (data not shown). We additionally evaluated the ability of these cells to attach to a plastic tissue culture dish. A substantially lower percentage of CD18/HPAF control cells attached to the plastic tissue culture dish surface compared with EIAS19 cells (Fig. 7*B*), suggesting an increase in adhesive properties of low MUC4-expressing cells. Also, the down-regulation of *MUC4* in antisense-transfected CD18/HPAF (EIAS19) cells resulted in enhanced aggregation compared with control cells (Fig. 7*C*).

HER2 Expression Is Down-Regulated in Antisense-MUC4 Construct-Transfected CD18/HPAF Cells. Studies conducted in our laboratory have shown that MUC4 and HER2 interact with each other and colocalize at the cell surface and in the cytoplasm (unpublished data). Detection of MUC4-HER2 complex in cytoplasm suggests that this interaction begins before their localization to the cell membrane. Recently, SMC/Muc4, the rat homologue of MUC4, has also been shown to interact with ErbB2/HER2/neu and induce its autophosphorylation (at Tyr^{1248}) and translocation from the basolateral to the apical surface in polarized human colon carcinoma CACO-2 cells (23). On the basis of these prior observations, we sought to examine whether *MUC4* down-regulation in CD18/HPAF cells would have an impact on HER2/neu. HER2 expression and phosphorylation were examined using anti-HER2 and antiphosphotyrosine^{1248}-HER2 antibodies. Fig. 8 shows a reduced level of total and phosphorylated (at Tyr^{1248}) HER2 protein in antisense MUC4-transfected cells compared with the other control cell lines. Furthermore, the diminished expression of HER2 was correlated with the knocked down MUC4 protein levels in the two antisense-MUC4 clones (EIAS19 and EAS8; Fig. 8), implicating a role of MUC4 mucin in HER2 gene regulation. Reduction in the phosphorylated form of HER2, however, may be an effect of the down-regulation of total HER2 protein as its level declines in parallel to that of the total HER2 protein (Fig. 8).

DISCUSSION

The present study was undertaken to analyze the role of the MUC4 mucin in pancreatic tumor development and progression. Mucins are generally known to protect surface epithelia from injuries and infections under normal physiological conditions but often display deregulated expression in malignant cells (4, 6, 10). We have previously reported that the human mucin gene *MUC4* is aberrantly expressed in

Table 1 *Growth of pancreatic tumors developed by orthotopic implantation of CD18/HPAF controls (parent, vector control ZEO, and sense control ES6) and antisense-MUC4-expressing (EIAS19) cells in immunodeficient mice*

Cell line	n	Median tumor weight (g)	Range	Median tumor volume (mm^3)	Range
CD18/HPAF	12	1.80	1.2–2.7	900	576–1513
ZEO	12	1.55	1.3–2.4	789	640–1513
ES6	12	1.60	1.2–2.2	789	576–1250
EIAS19	13	$0.90^{a,b,c}$	0.5–1.8	$512^{a,b,c}$	221–908

[a] $P = 0.01$ compared with CD18/HPAF.
[b] $P = 0.01$ compared with ZEO.
[c] $P = 0.01$ compared with ES6.

Table 2 *Incidences of metastases[a] of pancreatic tumors developed by orthotopic implantation of CD18/HPAF controls (detailed in Table 1) and antisense-MUC4-expressing (EIAS19) cells in immunodeficient mice*

Cell line	Lymph node	Diaphragm	Liver	Caecum	Lung
CD18/HPAF	10/12 (83%)	9/12 (75%)	2/12 (17%)	2/12 (17%)	1/12 (8%)
ZEO	12/12 (100%)	4/12 (33%)	3/12 (25%)	0/12 (0%)	0/12 (0%)
ES6	12/12 (100%)	3/12 (25%)	3/12 (25%)	0/12 (0%)	1/12 (8%)
EIAS19	4/13 (31%)[b,c,d]	0/13 (0%)[e,f]	0/13 (0%)	0/13 (0%)	0/12 (0%)

[a] No incidence of metastasis was observed for heart and kidneys in any of the group.
[b] $P = 0.02$ compared with CD18/HPAF.
[c] $P < 0.001$ compared with ZEO.
[d] $P < 0.001$ compared with ES6.
[e] $P < 0.001$ compared with CD18/HPAF.
[f] $P = 0.04$ compared with ZEO.

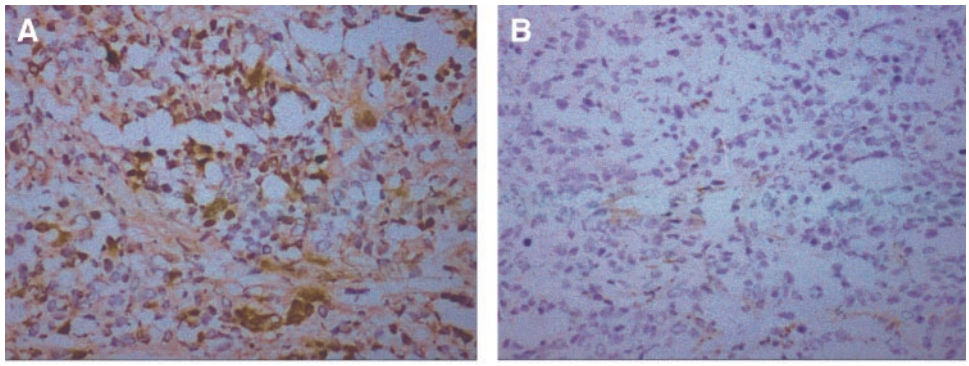

Fig. 6. Immunohistochemical analysis of primary tumors developed in immunodeficient mice by orthotopic implantation of ZEO (empty vector; *A*) and EIAS19 (antisense; *B*) CD18/HPAF cells. Tumor sections were stained for MUC4-positive cells using MUC4-specific monoclonal antibody followed by biotinylated secondary antibody incubation and a streptavidin peroxidase 3,3′-diaminobenzidine-chromogen detection system. The two panels represent ×100 magnifications. *B* (EIAS19) shows low signal intensity and tumor cell population compared with *A* (ZEO).

pancreatic tumors and cell lines but has no detectable expression in the normal pancreas (10). The present *in vitro* and *in vivo* data reveal that the silencing of *MUC4* expression results in altered tumor cell behavior, decreased growth, and a marked reduction in metastatic incidences in an orthotopic mouse model of pancreatic cancer. These results are in support of the previous observations and establish a direct association of *MUC4* expression with the disease development.

Down-regulating the expression is one of the convenient and reliable approaches for functional analyses of genes (reviewed in Refs. 29, 30). In the current study, we generated a stably transfected CD/HPAF cell clone (EIAS19) with greatly diminished expression of MUC4 protein as demonstrated by western and confocal microscopic analyses (Figs. 1 and 2). Control cell clones were also generated by stably transfecting empty vector and partial length sense-RNA construct to minimize the effect, if any, because of the foreign DNA integration into the host genome, expression of nonhost transcripts, and clone selection conditions. Antisense-RNA-based gene silencing strategy has been used efficiently to study the gene functions in human cells (31, 32); however, present work is the first report on *MUC4* mucin down-regulation using this approach.

Normal cell growth is maintained and modulated by positive (cell proliferative) and negative (apoptotic) signals. Loss of regulatory mechanisms as a consequence of either the loss of tumor suppressor gene function or deregulated tumor progressor gene function may contribute to the oncogenic process. The present study shows an enhanced population doubling time and, therefore, suppressed tumor cell growth in low MUC4-expressing EIAS19 cells (Fig. 4, *A* and *B*). The EIAS19 cells also showed a reduced clonogenic ability (Fig. 5) and suppressed tumor growth in immunodeficient mice compared with high MUC4-expressing control cell lines (Table 1). Therefore, our data indicate that MUC4 possesses a tumor progressor function in pancreatic cancer. The overexpression of SMC (rat homologue of

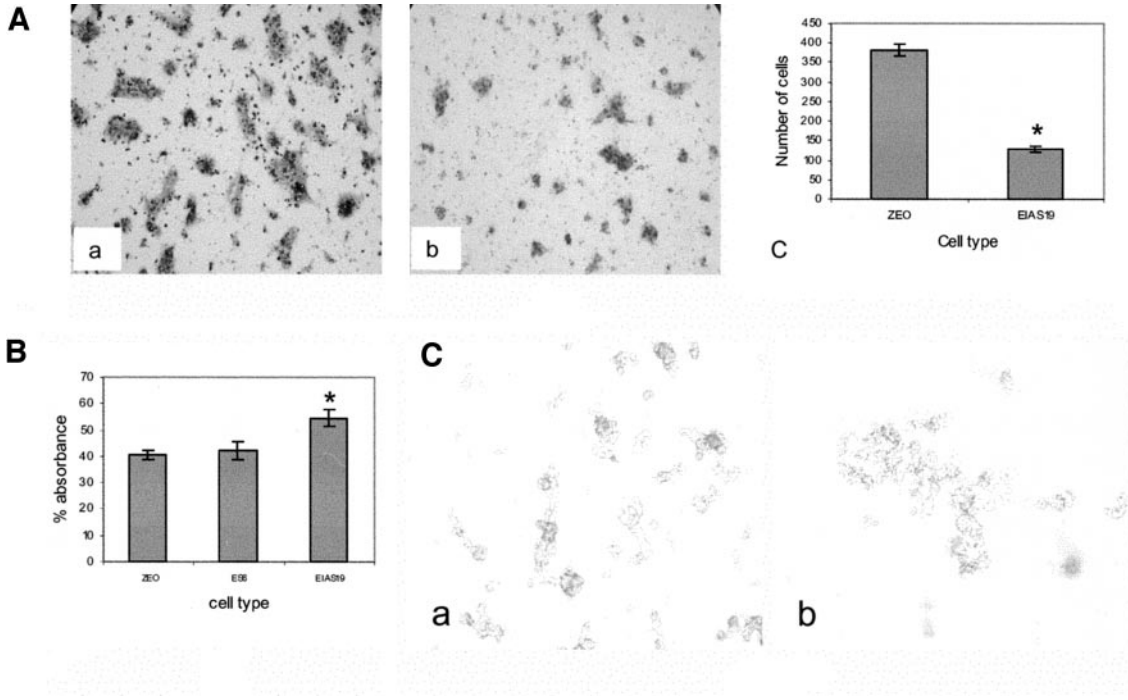

Fig. 7. Changes in tumor cell behavior of antisense-MUC4 expressing sub-line (EIAS19) compared with CD18/HPAF control cells. *A*, cell motility assay: MUC4 expression correlates with the cell motility. Cells were plated on noncoated membranes for motility assays. The cells were incubated for 24 h, and those that did not migrate through the pores in the membrane were removed by scraping the membrane with a cotton swab and the remaining cells were stained. Cell motility is more in ZEO (*a*) compared with EIAS19 (*b*) cells. *c*, the number of cells transversing the membrane was determined by averaging 10 random fields of view at ×100. The data are expressed as the number of cells/field of view and is the average of three independent experiments. *Error bars* indicate SE of the average (∗, $P < 0.05$). *B*, adhesion assay: cells were seeded in 24-well plates and incubated for 5 h. At this time, EIAS19 cells showed a significant increase (∗, $P < 0.05$) in the percentage of attached cells. Results are expressed as mean ± SE of four separate experiments. *C*, aggregation assay: 20-μl drops of medium containing 5000 cells/drop were pipetted onto the inner surface of the lid of a Petri dish. The lid was then placed on the Petri dish so that the drops were hanging from the lid with the cells suspended within them. After overnight incubation at 37°C, the lid of the Petri dish was inverted and photographed at ×40 magnification: *a*, ZEO (empty vector transfected); *b*, EIAS19 (antisense-MUC4 transfected). An increased cellular aggregation was observed in low MUC4-expressing EIAS19 cells.

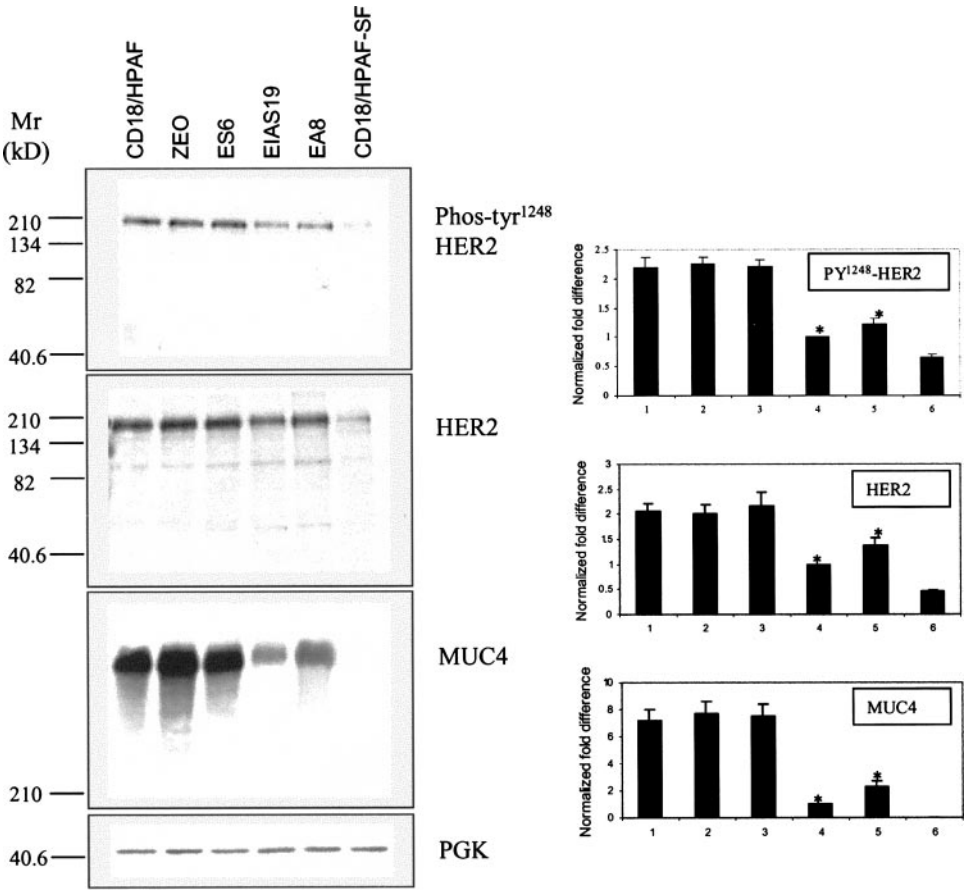

Fig. 8. Western blot analysis of HER2 expression and HER2 Tyr^{1248} phosphorylation in CD18/HPAF and derived sublines. The protein was isolated from subconfluent cultures and 10 μg of protein from each cell extract was resolved by SDS-PAGE (10%), transferred to the polyvinylidene difluoride membrane and probed with antibodies against HER2, phospho-tyr^{1248} HER2 and phosphoglycerol kinase (PGK; internal control). Antisense-MUC4-transfected (EIAS19 and EAS8) cells show down-regulated HER2 expression compared with other control cell lines resulting in an overall reduction of phosphorylated-HER2. *Bars* represent the normalized fold difference in total and phospho-tyr^{1248} HER2 protein levels (mean $\pm$ SE; $n = 3$, $*$, $P < 0.05$). The diminished MUC4 expression is directly correlated with the HER2 expression levels.

MUC4) has been reported to accelerate the growth of xeno-transplanted A375 melanoma in host animals via the suppression of apoptosis (7). SMC/Muc4 acts as an intramembrane ligand for ErbB2/HER2/neu and potentiates its autophosphorylation (33). It has been suggested that Muc4-induced ErbB2/neu signaling may mediate antiapoptotic function of SMC/Muc4 (7). In our study, antisense-MUC4 transfected cells showed a down-regulated expression of the HER2/neu protein, resulting in an overall reduction of phosphorylated HER2 (Fig. 8). HER2 has been implicated in cell proliferation via initiating signals for growth regulatory pathways (24, 34). Its expression and function has also been studied in pancreatic cancer cells and has been associated with cell proliferation and metastasis (35, 36). Taken together, these observations suggest that MUC4 may potentiate its tumor progressor function, at least in part, via regulating HER2 gene expression. Furthermore, MUC4-associated HER2 down-regulation in our model system indicates a novel feature of MUC4 in the regulation of gene expression, although the intricate molecular mechanism(s) are yet to be investigated. The interaction between MUC4 and HER2 and their colocalization have been demonstrated in pancreatic cancer cells (unpublished data). Furthermore, in a recent study, SMC/Muc4 has been shown to alter the localization of ErbB2/HER2 in human colon carcinoma CACO-2 cells, which suggests a strong physical association between the two molecules (23). Analysis of HER2 expression at RNA level showed no apparent changes among CD/HPAF control and antisense cell lines (unpublished observation), indicating that MUC4-mediated HER2 expression is regulated by posttranscriptional mechanism(s). The actual relevance of this observation is yet to be established in other MUC4-expressing pancreatic cancer cell lines; nevertheless, it points toward a functional significance of interaction between the MUC4 and HER2 proteins in pancreatic tumor biology.

In our study, the expression of *MUC4* also correlated with the incidences of tumor metastasis, suggesting a role of MUC4 in the potentiation of tumor metastasis. *In vivo* metastasis of tumor cells is an extremely complicated process that involves several consecutive events (*i.e.*, detachment of tumor cells from primary site, intravasation into blood stream, evasion of immune surveillance, adherence to vascular endothelial cells of distant organs, and finally extravasation into such tissues; Refs. 37, 38). During the initial process of tumor cell metastasis, the weakening of cell-matrix and cell-cell interactions is imperative for the detachment of tumor cells from primary sites. Membrane-bound mucins are considered to be the important determinants of the cell's adhesive properties and therefore of metastatic potential, even in cases where the level of known adhesion molecules remain unchanged (27, 28). Large cell surface mucins (500–2000 nm) confer their antiadhesive properties by stearically blocking the interaction of the surface adhesion molecules, which do not extend >30 nm over the cell surface, with their ligands in the extracellular matrix (39, 40). Overexpression of the cell surface *Muc4*/SMC has been reported to disrupt integrin-mediated cell adhesions as well as the homotypic cell-cell interactions, causing the dissociation of tumor cells in culture (22). Similarly, MUC1 has been implicated in determining the adhesion properties of cells, primarily through the modulation of integrin-mediated adhesion in melanoma cell lines (9). Furthermore, MUC1 overexpression suppresses the normal E-cadherin function in breast cancer cell lines (41, 42). MUC4 is a large molecule and its length is estimated to range between 1.1 and 2.1 μm, which is ~2–5 times greater than the approximated MUC1 size (500 nm; Ref. 17, 43). Therefore, considering its large size, a similar and more potent impact of MUC4 on adhesive properties of the cell can be predicted. Consistent with the proposed mechanism, the present data (Fig. 7, *B* and *C*) demonstrated enhanced adhesion and cell-cell aggregation in low MUC4-expressing EIAS19 cells. Furthermore,

EIAS19 cells also showed reduced cell motility in Boyden's chamber assay (Fig. 7*A*), hereby suggesting that MUC4 may also be implicated in cell motility. Cell motility is typically associated with the coordinated disassembly and reformation of the cortical actin network (44) and can partly be defined by the extracellular matrix composition and the expression levels of integrins and cadherins (45, 46). Although the published articles suggest a function of the MUC1 mucin in cell migration (8, 47), no information is available regarding any direct or indirect impact of MUC4 on cell motility or motility-related proteins. In consideration of the present finding, however, it will be interesting to investigate the mechanism(s) by which MUC4 influences the motile properties of the cells.

In many studies, the tumor progression has been shown to be associated with the altered glycosylation of cell surface proteins (48, 49). Glycosylated mucins expressed on the tumor cell surface can promote metastasis via selectin-mediated mechanisms, which help in the adhesion of tumor cells to secondary sites (50, 51). There is no published data available on the interaction of MUC4 with the selectin family of adhesion molecules; however, this possibility cannot be excluded and needs to be explored. Furthermore, the expression levels of ErbB2/HER2 have also been correlated with the tumor size and metastasis of the tumor to lymph nodes, implying the involvement of ErbB2 and ErbB2-mediated signals in tumorigenesis (52). The engagement of cell-surface receptors by a ligand regulates a number of biological processes. These processes induce cell cycle progression, cell migration, cell metabolism and survival, as well as cell proliferation and differentiation (53, 54). Hence, considering these observations, the down-regulation of HER2 in low MUC4-expressing cells may also be an important determinant of a less malignant phenotype of tumor cells, apart from any direct impact of MUC4 on tumor cell behavior and metastasis.

In conclusion, we propose that MUC4 is implicated in tumor growth and metastasis by directly altering the tumor cell properties (adhesion/aggregation and motility) and/or, in part, via modulating HER2 expression. The present work is the first demonstration of the direct association of MUC4 with the metastatic pancreatic cancer phenotype. Moreover, it provides evidence for the functional role of MUC4 in tumor cell growth and behavior and suggests a critical role of *MUC4* up-regulation in pancreatic adenocarcinoma.

ACKNOWLEDGMENTS

We thank Erik Moore for technical support, the Molecular Biology Core Facility, University of Nebraska Medical Center, for oligonucleotide synthesis and DNA sequencing, Monoclonal Antibody Core Facility, and Kristi L. W. Berger (Eppley Institute) for editorial assistance. We also thank Dr. Parmender Mehta (Department of Biochemistry and Molecular Biology) and Dr. Rakesh Singh (Department of Pathology and Microbiology) at University of Nebraska Medical Center for critical reading of the manuscript.

REFERENCES

1. el-Kamar, F. G., Grossbard, M. L., and Kozuch, P. S. Metastatic pancreatic cancer: emerging strategies in chemotherapy and palliative care. Oncologist, *8:* 18–34, 2003.
2. Evans, D. B., Abbruzzese, J. L., and Willett, C. G. Cancer of the pancreas. *In*: S. Hellman, S. A. Rosenberg, and V. T. DeVita (eds.), Cancer: Principles and Practice of Oncology, 6th ed., pp. 1126–1161. Philadelphia: Lippincott Williams and Wilkins, 2001.
3. Fernandez, E., La Vecchia, C., Porta, M., Negri, E., Lucchini, F., and Levi, F. Trends in pancreatic cancer mortality in Europe, 1955–1989. Int. J. Cancer, *57:* 786–792, 1994.
4. Strous, G. J., and Dekker, J. Mucin-type glycoproteins. Crit. Rev. Biochem. Mol. Biol., *27:* 57–92, 1992.
5. Moniaux, N., Escande, F., Porchet, N., Aubert, J. P., and Batra, S. K. Structural organization and classification of the human mucin genes. Front. Biosci., *6:* D1192–D1206, 2001.
6. Gendler, S. J., and Spicer, A. P. Epithelial mucin genes. Annu. Rev. Physiol., *57:* 607–634, 1995.
7. Komatsu, M., Jepson, S., Arango, M. E., Carothers Carraway, C. A., and Carraway, K. L. Muc4/sialomucin complex, an intramembrane modulator of ErbB2/HER2/Neu, potentiates primary tumor growth and suppresses apoptosis in a xenotransplanted tumor. Oncogene, *20:* 461–470, 2001.
8. Satoh, S., Hinoda, Y., Hayashi, T., Burdick, M. D., Imai, K., and Hollingsworth, M. A. Enhancement of metastatic properties of pancreatic cancer cells by MUC1 gene encoding an anti-adhesion molecule. Int. J. Cancer, *88:* 507–518, 2000.
9. Wesseling, J., van der Valk, S. W., Vos, H. L., Sonnenberg, A., and Hilkens, J. Episialin (MUC1) overexpression inhibits integrin-mediated cell adhesion to extracellular matrix components. J. Cell Biol., *129:* 255–265, 1995.
10. Andrianifahanana, M., Moniaux, N., Schmied, B. M., Ringel, J., Friess, H., Hollingsworth, M. A., Buchler, M. W., Aubert, J. P., and Batra, S. K. Mucin (MUC) gene expression in human pancreatic adenocarcinoma and chronic pancreatitis: a potential role of MUC4 as a tumor marker of diagnostic significance. Clin. Cancer Res., *7:* 4033–4040, 2001.
11. Swartz, M. J., Batra, S. K., Varshney, G. C., Hollingsworth, M. A., Yeo, C. J., Cameron, J. L., Wilentz, R. E., Hruban, R. H., and Argani, P. MUC4 expression increases progressively in pancreatic intraepithelial neoplasia. Am. J. Clin. Pathol., *117:* 791–796, 2002.
12. Park, H. U., Kim, J. W., Kim, G. E., Bae, H. I., Crawley, S. C., Yang, S. C., Gum, J., Jr., Batra, S. K., Rousseau, K., Swallow, D. M., Sleisenger, M. H., and Kim, Y. S. Aberrant expression of MUC3 and MUC4 membrane-associated mucins and sialyl lex antigen in pancreatic intraepithelial neoplasia. Pancreas, *26:* E48–E54, 2003.
13. Lopez-Ferrer, A., Alameda, F., Barranco, C., Garrido, M., and de Bolos, C. MUC4 expression is increased in dysplastic cervical disorders. Hum. Pathol., *32:* 1197–1202, 2001.
14. Lee, K. T., and Liu, T. S. Altered mucin gene expression in stone-containing intrahepatic bile ducts and cholangiocarcinomas. Dig. Dis. Sci., *46:* 2166–2172, 2001.
15. Hanaoka, J., Kontani, K., Sawai, S., Ichinose, M., Tezuka, N., Inoue, S., Fujino, S., and Ohkubo, I. Analysis of MUC4 mucin expression in lung carcinoma cells and its immunogenicity. Cancer (Phila.), *92:* 2148–2157, 2001.
16. Nguyen, P. L., Niehans, G. A., Cherwitz, D. L., Kim, Y. S., and Ho, S. B. Membrane-bound (MUC1) and secretory (MUC2, MUC3, and MUC4) mucin gene expression in human lung cancer. Tumour Biol., *17:* 176–192, 1996.
17. Moniaux, N., Nollet, S., Porchet, N., Degand, P., Laine, A., and Aubert, J. P. Complete sequence of the human mucin MUC4: a putative cell membrane-associated mucin. Biochem. J., *338:* 325–333, 1999.
18. Nollet, S., Moniaux, N., Maury, J., Petitprez, D., Degand, P., Laine, A., Porchet, N., and Aubert, J. P. Human mucin gene MUC4: organization of its 5′-region and polymorphism of its central tandem repeat array. Biochem. J., *332:* 739–748, 1998.
19. Choudhury, A., Moniaux, N., Winpenny, J. P., Hollingsworth, M. A., Aubert, J. P., and Batra, S. K. Human MUC4 mucin cDNA and its variants in pancreatic carcinoma. J. Biochem., *128:* 233–243, 2000.
20. Komatsu, M., Yee, L., and Carraway, K. L. Overexpression of sialomucin complex, a rat homologue of MUC4, inhibits tumor killing by lymphokine-activated killer cells. Cancer Res., *59:* 2229–2236, 1999.
21. Komatsu, M., Tatum, L., Altman, N. H., Carothers Carraway, C. A., and Carraway, K. L. Potentiation of metastasis by cell surface sialomucin complex (rat MUC4), a multifunctional anti-adhesive glycoprotein. Int. J. Cancer, *87:* 480–486, 2000.
22. Komatsu, M., Carraway, C. A., Fregien, N. L., and Carraway, K. L. Reversible disruption of cell-matrix and cell-cell interactions by overexpression of sialomucin complex. J. Biol. Chem., *272:* 33245–33254, 1997.
23. Ramsauer, V. P., Carothers Carraway, C. A., Salas, P. J., and Carraway, K. L. Muc4/Sialomucin complex, the intramembrane ErbB2 ligand, translocates ErbB2 to the apical surface in polarized epithelial cells. J. Biol. Chem., *278:* 30142–30147, 2003.
24. Goebel, S. U., Iwamoto, M., Raffeld, M., Gibril, F., Hou, W., Serrano, J., and Jensen, R. T. Her-2/neu expression and gene amplification in gastrinomas: correlations with tumor biology, growth, and aggressiveness. Cancer Res., *62:* 3702–3710, 2002.
25. Choudhury, A., Singh, R. K., Moniaux, N., El Metwally, T. H., Aubert, J. P., and Batra, S. K. Retinoic acid-dependent transforming growth factor-β 2-mediated induction of MUC4 mucin expression in human pancreatic tumor cells follows retinoic acid receptor-α signaling pathway. J. Biol. Chem., *275:* 33929–33936, 2000.
26. Zhang, Y., Zhao, W., Zhang, H. J., Domann, F. E., and Oberley, L. W. Overexpression of copper zinc superoxide dismutase suppresses human glioma cell growth. Cancer Res., *62:* 1205–1212, 2002.
27. Sommers, C. L. The role of cadherin-mediated adhesion in breast cancer. J. Mammary Gland Biol. Neoplasia, *1:* 219–229, 1996.
28. Truant, S., Bruyneel, E., Gouyer, V., De Wever, O., Pruvot, F. R., Mareel, M., and Huet, G. Requirement of both mucins and proteoglycans in cell-cell dissociation and invasiveness of colon carcinoma HT-29 cells. Int. J. Cancer, *104:* 683–694, 2003.
29. Yin, D., and Ji, Y. Genomic analysis using conditional phenotypes generated by antisense RNA. Curr. Opin. Microbiol., *5:* 330–333, 2002.
30. Schuch, W. Using antisense RNA to study gene function. Symp. Soc. Exp. Biol., *45:* 117–127, 1991.
31. Wojnar, P., Lechner, M., and Redl, B. Antisense down-regulation of lipocalin-interacting membrane receptor expression inhibits cellular internalization of lipocalin-1 in human NT2 cells. J. Biol. Chem., *278:* 16209–16215, 2003.
32. Vilenchik, M., Raffo, A. J., Benimetskaya, L., Shames, D., and Stein, C. A. Antisense RNA down-regulation of bcl-xL expression in prostate cancer cells leads to diminished rates of cellular proliferation and resistance to cytotoxic chemotherapeutic agents. Cancer Res., *62:* 2175–2183, 2002.
33. Carraway, K. L., Perez, A., Idris, N., Jepson, S., Arango, M., Komatsu, M., Haq, B., Price-Schiavi, S. A., Zhang, J., and Carraway, C. A. Muc4/sialomucin complex, the

intramembrane ErbB2 ligand, in cancer and epithelia: to protect and to survive. Prog. Nucleic Acid Res. Mol. Biol., *71:* 149–185, 2002.
34. Slamon, D. J., Clark, G. M., Wong, S. G., Levin, W. J., Ullrich, A., and McGuire, W. L. Human breast cancer: correlation of relapse and survival with amplification of the HER-2/neu oncogene. Science (Wash. DC), *235:* 177–182, 1987.
35. Lei, S., Appert, H. E., Nakata, B., Domenico, D. R., Kim, K., and Howard, J. M. Overexpression of HER2/neu oncogene in pancreatic cancer correlates with shortened survival. Int. J. Pancreatol., *17:* 15–21, 1995.
36. Thybusch-Bernhardt, A., Aigner, A., Beckmann, S., Czubayko, F., and Juhl, H. Ribozyme targeting of HER-2 inhibits pancreatic cancer cell growth *in vivo*. Eur. J. Cancer, *37:* 1688–1694, 2001.
37. Fidler, I. J. Critical factors in the biology of human cancer metastasis: Twenty-Eighth G. H. A. Clowes Memorial Award Lecture. Cancer Res., *50:* 6130–6138, 1990.
38. Folkman, J. Endothelial cells and angiogenic growth factors in cancer growth and metastasis. Introduction. Cancer Metastasis Rev., *9:* 171–174, 1990.
39. Becker, J. W., Erickson, H. P., Hoffman, S., Cunningham, B. A., and Edelman, G. M. Topology of cell adhesion molecules. Proc. Natl. Acad. Sci. USA, *86:* 1088–1092, 1989.
40. Codington, J. F., and Frim, D. M. Cell-surface macromolecular and morphological changes related to allotransplantability in the TA3 tumor. Biomembranes, *11:* 207–258, 1983.
41. Kondo, K., Kohno, N., Yokoyama, A., and Hiwada, K. Decreased MUC1 expression induces E-cadherin-mediated cell adhesion of breast cancer cell lines. Cancer Res., *58:* 2014–2019, 1998.
42. Wesseling, J., van der Valk, S. W., and Hilkens, J. A mechanism for inhibition of E-cadherin-mediated cell-cell adhesion by the membrane-associated mucin episialin/MUC1. Mol. Biol. Cell, *7:* 565–577, 1996.
43. Jentoft, N. Why are proteins *O*-glycosylated? Trends Biochem. Sci., *15:* 291–294, 1990.
44. Cunningham, C. C. Actin structural proteins in cell motility. Cancer Metastasis Rev., *11:* 69–77, 1992.
45. Chen, H., Paradies, N. E., Fedor-Chaiken, M., and Brackenbury, R. E-Cadherin mediates adhesion and suppresses cell motility via distinct mechanisms. J. Cell Sci., *110:* 345–356, 1997.
46. Palecek, S. P., Loftus, J. C., Ginsberg, M. H., Lauffenburger, D. A., and Horwitz, A. F. Integrin-ligand binding properties govern cell migration speed through cell-substratum adhesiveness. Nature (Lond.), *385:* 537–540, 1997.
47. Correa, I., Plunkett, T., Vlad, A., Mungul, A., Candelora-Kettel, J., Burchell, J. M., Taylor-Papadimitriou, J., and Finn, O. J. Form and pattern of MUC1 expression on T cells activated *in vivo* or *in vitro* suggests a function in T-cell migration. Immunology, *108:* 32–41, 2003.
48. Kim, Y. J., and Varki, A. Perspectives on the significance of altered glycosylation of glycoproteins in cancer. Glycoconj. J., *14:* 569–576, 1997.
49. Kim, Y. S., Gum, J., Jr., and Brockhausen, I. Mucin glycoproteins in neoplasia. Glycoconj. J., *13:* 693–707, 1996.
50. Borsig, L., Wong, R., Hynes, R. O., Varki, N. M., and Varki, A. Synergistic effects of L- and P-selectin in facilitating tumor metastasis can involve non-mucin ligands and implicate leukocytes as enhancers of metastasis. Proc. Natl. Acad. Sci. USA, *99:* 2193–2198, 2002.
51. Mannori, G., Crottet, P., Cecconi, O., Hanasaki, K., Aruffo, A., Nelson, R. M., Varki, A., and Bevilacqua, M. P. Differential colon cancer cell adhesion to E-, P-, and L-selectin: role of mucin-type glycoproteins. Cancer Res., *55:* 4425–4431, 1995.
52. Yu, D., and Hung, M. C. Overexpression of ErbB2 in cancer and ErbB2-targeting strategies. Oncogene, *19:* 6115–6121, 2000.
53. Yamasaki, S., Nishida, K., Yoshida, Y., Itoh, M., Hibi, M., and Hirano, T. Gab1 is required for EGF receptor signaling and the transformation by activated ErbB2. Oncogene, *22:* 1546–1556, 2003.
54. Fiorentino, L., Pertica, C., Fiorini, M., Talora, C., Crescenzi, M., Castellani, L., Alema, S., Benedetti, P., and Segatto, O. Inhibition of ErbB-2 mitogenic and transforming activity by RALT, a mitogen-induced signal transducer which binds to the ErbB-2 kinase domain. Mol. Cell. Biol., *20:* 7735–7750, 2000.